Gas-Phase Acid-Base Properties of Melamine and Cyanuric Acid

Sumit Mukherjee and Jianhua Ren
Department of Chemistry, University of the Pacific, Stockton, California, USA

The thermochemical properties of melamine and cyanuric acid were characterized using mass spectrometry measurements along with computational studies. A triple-quadrupole mass spectrometer was employed with the application of the extended Cooks kinetic method. The proton affinity (*PA*), gas-phase basicity (*GB*), and protonation entropy ($\Delta_p S$) of melamine were determined to be 226.2 ± 2.0 kcal/mol, 218.4 ± 2.0 kcal/mol, and 26.2 ± 2.0 cal/mol K, respectively. The deprotonation enthalpy ($\Delta_{acid}H$), gas-phase acidity ($\Delta_{acid}G$), and deprotonation entropy ($\Delta_{acid}S$) of cyanuric acid were determined to be 330.7 ± 2.0 kcal/mol, 322.9 ± 2.0 kcal/mol, and 26.1 ± 2.0 cal/mol K, respectively. The geometries and energetics of melamine, cyanuric acid, and related ionic species were calculated at the B3LYP/6-31+G(d) level of theory. The computationally predicted proton affinity of melamine (225.9 kcal/mol) and gas-phase deprotonation enthalpy of cyanuric acid (328.4 kcal/mol) agree well with the experimental results. Melamine is best represented as the imide-like triazine-triamine form and the triazine nitrogen is more basic than the amino group nitrogen. Cyanuric acid is best represented as the keto-like tautomer and the N-H group is the most probable proton donor. (J Am Soc Mass Spectrom 2010, 21, 1720–1729) © 2010 American Society for Mass Spectrometry

Melamine (MEL) is a triazine-derivative and may be described by two structural isomers, the imide-like triazine-triamine [1] and the amide-like tautomer [2]. Cyanuric acid (CYA) is also a triazine-derivative and may also be described as two structural isomers, the enol-like triazine-triol and the keto-like tautomer. Although MEL and CYA both share a triazine framework, they have quite different reactivity.

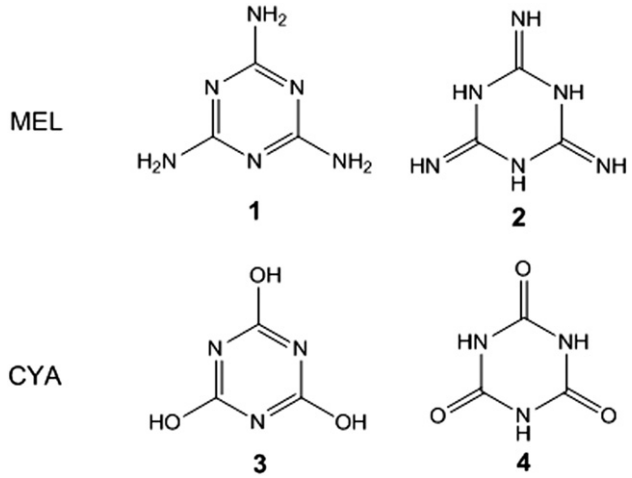

Both MEL and CYA are important industrial chemicals. MEL is used as a monomer to make thermosetting polymers, is one of the major colorant components in inks and plastics, and is an ingredient in flame-retardants [1–5]. MEL is also a metabolic byproduct or photo-degradation product of cyromazine, where cyromazine is used as a pesticide for plants [6, 7]. MEL has a high nitrogen content (66%), which had been misused as a fertilizer [8]. CYA is commonly used as a component of bleaches in swimming pools [9, 10]. MEL and CYA are both soluble in water. When combined, they form an insoluble crystal. The crystal is the result of the formation of a complex between MEL and CYA connected through an extended two-dimensional hydrogen-bonding network [11]. Under controlled conditions, MEL and CYA as well as their derivatives can form hydrogen-bonded self-assemblies with specific surface structures, and these assemblies have been used as surface templates in supramolecular chemistry [12–15]. The formation of the MEL–CYA complex is believed to be the main cause for kidney failure in children and pet animals when they consume tainted food [16–18].

In recent years, many analytical methods have been developed to detect trace amount of MEL and CYA in potentially contaminated food. This includes mass spectrometry-based methods [19–24], surface-enhanced Raman spectrometry applications [25], and other chemical methods [26]. In fact, all major mass spectrometer vendors use the detection of MEL and CYA as cases to demonstrate their instruments' performances [27–31]. All mass spectrometry methods require that MEL and CYA are being ionized in the gas phase. The efficiency of formation of charged MEL and CYA is directly related to the acid-base properties.

Address reprint requests to Dr. J. Ren, Department of Chemistry, University of the Pacific, 3601 Pacific Ave., Stockton, CA 95211, USA. E-mail: jren@pacific.edu

1044-0305/10/$32.00
doi:10.1016/j.jasms.2010.06.002

Published online June 11, 2010
Received April 19, 2010
Revised June 1, 2010
Accepted June 4, 2010

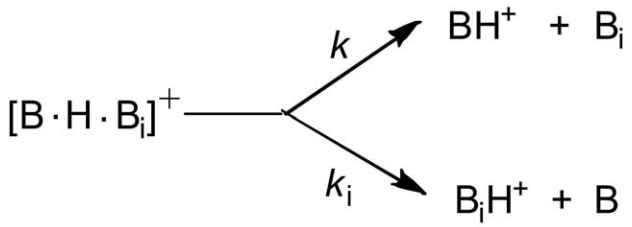

Scheme 1

Although the thermochemical properties of MEL and CYA have been investigated in the condensed phase, the gas-phase studies are very limited [32–35]. Some important questions regarding the intrinsic properties of these two compounds remain unanswered. MEL and CYA are a base and an acid, respectively. What are the quantitative values of the basicity and acidity? Which group is the most likely protonation or deprotonation site? Can MEL function as an acid and CYA function as a base as well? What are the most favored structures of MEL and CYA in the gas phase? In this paper, we describe the mass spectrometry measurements and computational studies of the gas-phase acid-base properties and the structural features of MEL and CYA.

Experimental

The Kinetic Method

The gas-phase basicity of melamine and the gas-phase acidity of cyanuric acid were determined using mass spectrometry techniques with the application of the extended Cooks kinetic method [36–39]. The Cooks kinetic method has been widely used to determine thermochemical properties of gas-phase neutral molecules and ions [40–50]. The gas-phase basicity (GB) of a base, B, is defined as the Gibbs free-energy change for the reaction $BH^+ \rightarrow B + H^+$. The proton affinity (PA) and the protonation entropy (Δ_pS) of B are the enthalpy and entropy changes for the same reaction, respectively. The gas-phase acidity ($\Delta_{acid}G$) of an acid HA is defined as the Gibbs free-energy change for the reaction $AH \rightarrow A^- + H^+$. The corresponding enthalpy and entropy changes are referred to as the gas-phase deprotonation enthalpy ($\Delta_{acid}H$) and deprotonation entropy ($\Delta_{acid}S$), respectively.

For measuring the PA of a basic species, B, a proton-bound heterodimer, $[B{\cdot}H{\cdot}B_i]^+$ is generated in the gas phase, where B_i is a group of reference bases with known PA values. The proton-bound dimer ions are accelerated and undergo collision-induced dissociation (CID) in the collision cell. Ideally, the energized dimer ions will fragment to yield two product ions, BH^+ and B_iH^+, with rate constant k and k_i, Scheme 1. If the secondary fragment ions are negligible, the ratio of the rate constants, k/k_i, can be assumed to be the ratio of the CID fragment ions, $[BH^+]/[B_iH^+]$. With the assumption that there are no reverse activation barriers, the gas-phase basicities of B and B_i are related by a linear equation, eq 1, where R is the universal gas constant and T_{eff} is called the "effective temperature" [51–54]. To evaluate the entropy contribution, the gas phase basicity is replaced by proton affinity according to the thermodynamic relationship, $GB = PA - T_{eff}(\Delta_pS)$. The term $\Delta(\Delta S)$ is the difference of the activation entropies between the two competing dissociation channels, $\Delta(\Delta_pS) = \Delta S^{\neq}(k) - \Delta S^{\neq}(k_i)$. If the reference bases all have similar structures, then the term $\Delta(\Delta S)$ can be assumed to be constant. Under the assumption of the negligible reverse activation barrier, $\Delta(\Delta S)$ can be calculated using the protonation entropies of the two bases (B and B_i), $\Delta(\Delta S) \approx \Delta_pS - \Delta_pS_i$. To have a proper statistical treatment of the uncertainty throughout the data analysis, the average proton affinity of the reference acids, PA_{avg}, was introduced and eq 1 was converted to eq 2, where $\ln([BH^+]/[B_iH^+])$ has a linear relationship with $PA_{Bi} - PA_{avg}$ [55, 56].

The proton affinity of B can be derived from two sets of thermo-kinetic plots based on eq 2. The first set consists of the linear plot of $\ln([BH^+]/[B_iH^+])$ against $PA_{Bi} - PA_{avg}$. The slope will be $-1/RT_{eff}$ and the y-intercept will be $[(PA_B - PA_{avg})/RT_{eff} - \Delta(\Delta S)/R]$. If the CID experiments are carried out at several collision energies, a set of linear plots with different slopes and intercepts will be obtained. The group of slopes and intercepts will be used to construct the second set of the thermo-kinetic plot by plotting the values of $y = [(PA_B - PA_{avg})/RT_{eff} - \Delta(\Delta S)/R]$ against $1/RT_{eff}$. The slope will be $PA_B - PA_{avg}$, and the y-intercept will be $-\Delta(\Delta S)/R$. Since PA_{avg} is a known value, PA_B as well as the entropy term ($\Delta(\Delta S)$) can then be obtained. The protonation entropy of B can be calculated using the equation, $\Delta_pS_B = \Delta(\Delta S) + \Delta_pS_{Bi}$. Since protonation entropy varies slightly from one reference base to the other, the average entropy (Δ_pS_{avg}) of the reference bases can be used as the value of Δ_pS_{Bi}. With the protonation enthalpy and entropy available, the gas-phase basicity of B can be calculated using eq 3, where $T = 298$ K.

$$In\left(\frac{k}{k_i}\right) = \frac{GB_B - GB_{Bi}}{RT_{eff}} = \frac{PA_{Bi} - PA_B}{RT_{eff}} + \frac{\Delta(\Delta S)}{R}$$

$$\text{where } \frac{k}{k_i} \approx \frac{[BH^+]}{[B_iH^+]} \quad \text{and} \quad \Delta(\Delta S) \approx \Delta_pS_B - \Delta_pS_{Bi} \qquad (1)$$

$$In\left(\frac{[BH^+]}{[B_iH^+]}\right) = -\frac{PA_{Bi} - PA_{avg}}{RT_{eff}} + \left[\frac{PA_B - PA_{avg}}{RT_{eff}} - \frac{\Delta(\Delta S)}{R}\right] \qquad (2)$$

$$GB = PA - T(\Delta_pS) \qquad (3)$$

For measuring the acidity, a proton-bound heterodimer, $[A{\cdot}H{\cdot}A_i]^-$, is generated in the gas-phase, where A_iH is a group of reference acids with known gas-phase acidities and deprotonation enthalpies. Upon the CID exper-

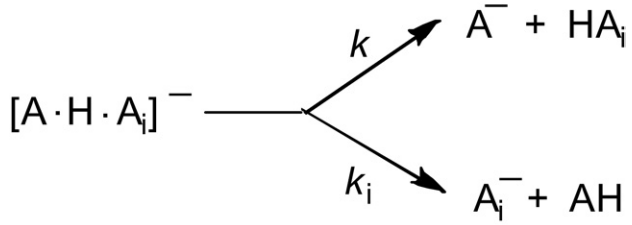

Scheme 2

iments, the dimer ions dissociate into two product ions, A^- and A_i^-, with rate constant k and k_i, Scheme **2**. With the similar considerations as those for the proton affinity measurements, the acid deprotonation enthalpies of AH ($\Delta_{acid}H$) and A_iH ($\Delta_{acid}H_i$), and the CID product ion ratio, $[A^-]/[A_i^-]$, are related by a linear equation, eq 4, where $\Delta_{acid}H_{avg}$ is the average deprotonation enthalpy of the reference acids (A_iH) and $\Delta(\Delta S)$ can be treated as the difference in the deprotonation entropies of the two acids, $\Delta(\Delta S) \approx \Delta_{acid}S - \Delta_{acid}S_i$. The deprotonation enthalpy of AH can be derived from two sets of thermo-kinetic plots. The first set involves plotting $\ln([A^-]/[A_i^-])$ against $\Delta_{acid}H_i - \Delta_{acid}H_{avg}$, and the second set involves plotting $y = [(\Delta_{acid}H - \Delta_{acid}H_{avg})/RT_{eff} - \Delta(\Delta S)/R]$ against $1/RT_{eff}$. The values of $\Delta_{acid}H$ and $\Delta(\Delta S)$ are obtained from the slope and the intercept of the second plot, respectively. By assuming that $\Delta_{acid}S_i$ equals the average deprotonation entropy ($\Delta_{acid}S_{avg}$) of the reference acids, the deprotonation entropy ($\Delta_{acid}S$) of AH can also be obtained. Finally, the gas-phase acidity of AH can be derived from eq 5.

$$In(\frac{A^-}{A_i^-}) = \frac{\Delta_{acid}H_i - \Delta_{acid}H_{avg}}{RT_{eff}} - \left[\frac{\Delta_{acid}H - \Delta_{acid}H_{avg}}{RT_{eff}} - \frac{\Delta(\Delta S)}{R}\right] \quad (4)$$

$$\Delta_{acid}G = \Delta_{acid}H - T(\Delta_{acid}S) \quad (5)$$

The uncertainties of the average proton affinity (PA_{avg}) and deprotonation enthalpy ($\Delta_{acid}H_{avg}$) were calculated as the root sum square of the random and systematic errors. For a set of six reference bases, the random error was treated as the averaged uncertainty of the reference bases (±2.0 kcal/mol) divided by the square root of the number of the reference acids, $(2.0/\sqrt{6}) = 0.82$ kcal/mol, and the systematic error was assigned as $\sqrt{2.0} = 1.4$ kcal/mol. The root sum square of the random and systematic errors yielded $\sqrt{(0.82^2 + 1.4^2} = 1.6$ kcal/mol.

Mass Spectrometry Measurements

All experiments were carried out in a triple-quadrupole mass spectrometer with an electrospray ionization (ESI) source (Varian 1200 L; Varian Inc., Walnut Creek, CA, USA) located in the Mass Spectrometry Facility in the Chemistry Department of the University of the Pacific. Nitrogen was used as the desolvation gas and the drying gas temperature was set at 100–150 °C. The ion source was kept at 50 °C. The hexapole ion guide chamber has about 1 mTorr nitrogen gas. Ions generated in the ESI source are presumed to be thermalized by multiple collisions with the nitrogen molecules in the ion guide chamber. The CID experiments were performed by isolating the proton-bound heterodimeric ions with the first quadrupole with a peak width of ~1.0–1.2 (instrument parameter), adjusted to maximize ion signal while still maintaining sufficient resolution. The isolated ions were allowed to collide with argon atoms leaked into the collision chamber at a pressure of 0.40 ± 0.03 mTorr. The dissociation product ions were analyzed with the third quadrupole with a peak with of ~1.2. For the proton affinity measurements, the instrument was set in the positive ion mode. Nitrogen was used as the nebulizing gas. The ESI needle voltage was maintained at 5.0 kV and the capillary voltage was kept at about 15 V. The capillary voltage was found to be critical in forming proton-bound dimer ions. For the gas-phase acidity measurements, the instrument was set in the negative ion mode and compressed air was used as the nebulizing gas. The ESI needle voltage was maintained at −4.5 kV and the capillary voltage was kept at −20 to −40 V.

The CID spectra were initially recorded at several collision energies with the *m/z* range wide enough to cover all possible secondary fragments. The CID product ion intensities were measured by setting the instrument in the selected reaction monitoring (SRM) mode in which the scan was focused on selected product ions. All fragment ions resulting from the isolated proton-bound dimer ions were recorded in a single data acquisition process, lasting typically for ~5 min. Each acquisition was repeated three times in 1 d. Multiple measurements were performed on different days and the results were repeatable with a relative uncertainty of around ±5%. The CID experiments were performed at five different collision energies, corresponding to the center-of-mass energies (E_{cm}) of 1.0, 1.5, 2.0, 2.5, and 3.0 eV, respectively. The center-of-mass energy was calculated using the equation: $E_{cm} = E_{lab}$ [m/(M + m)], where E_{lab} is the collision energy in laboratory frame, m is the mass of argon, and M is the mass of the proton-bound dimer ion.

Chemicals

MEL was purchased from Alfa Aesar (Ward Hill, MA, USA) and CYA was purchased from Acros Organics (Morris Plains, NJ, USA). All other compounds were purchased from Sigma-Aldrich (St. Louis, MO, USA). All chemicals were used without further purification. Stock solutions (~10^{-3} M) of MEL, CYA, all reference bases, and reference acids were made up in HPLC-

Table 1. Thermochemical quantities of the reference bases used for the melamine system

Reference base	*PA*[a] (kcal/mol)	*GB*[a] (kcal/mol)	Δ_pS[b] (cal/mol.K)
Cyclohexylamine	223.3	215.0	27.9
t-Butylamine	223.3	215.1	27.5
Pyrrolidine	226.6	218.8	26.2
Diethylamine	227.6	219.7	26.5
Piperidine	228.0	220.0	26.8
Dibutylamine	231.5	223.5	26.8
	PA_{avg} = 226.7 ± 1.6[c]		Δ_pS_{avg} = 26.9 ± 1.6[d]

[a]Obtained from the NIST Chemistry Webbook [63]. All PA and GB values are assumed to have 2.0 kcal/mol of uncertainty.
[b]Derived from *PA* and *GB*: $GB = PA - T(\Delta_pS)$, where T = 298 K and Δ_pS is assumed to have 2.0 cal/mol K uncertainty.
[c]Average proton affinity of the set of reference bases.
[d]Average protonation entropy of the set of reference bases.

grade methanol and water with a 50:50 (vol:vol) ratio. The stock solution of MEL or CYA was mixed with that of a reference compound in appropriate volume ratios and the mixture was further diluted with methanol and water (50:50) to achieve a final concentration of 10^{-4}–10^{-5} M to be used as the sample solution. The sample solution was introduced into the ESI source by an infusion pump at a flow rate of 10 μL/min.

Computational Method

All computational studies were carried out using the Gaussian W03 suite of programs [57]. Geometry optimizations, frequency, and energy calculations were performed with density functional theory (DFT) at the B3LYP/6-31+G(d) level [58–61]. For each molecular species, the true energy minimum was confirmed by the absence of any imaginary frequency. The theoretical proton affinity of MEL and the gas-phase deprotonation enthalpy of CYA were calculated using the isodesmic proton transfer reactions, eqs 6 and 7, where B_i and A_iH are reference base and reference acid, respectively.

$$MELH^+ + B_i \rightarrow MEL + B_iH^+ \quad (6)$$

$$[CYA\text{-}H]^- + A_iH \rightarrow CYA + A_i^- \quad (7)$$

Results

Experimental Results for Melamine

Six amine bases (B_i) with proton affinities ranging from 223 to 231 kcal/mol were chosen as the references: cyclohexylamine, *t*-butylamine, pyrrolidine, diethylamine, piperidine, and dibutylamine, Table 1. The relative proton affinity of MEL was examined by using CID-bracketing experiments. The relative CID product ion intensities should reveal the relative proton affinity between that of MEL and the reference base that forms the proton-bound dimer with MEL. The CID spectra (Figure 1) show that the ion intensity of protonated MEL is stronger than that of protonated *t*-butylamine and weaker than that of protonated pyrrolidine, revealing that the proton affinity of MEL is between those of the two references.

The quantitative proton affinity of MEL was measured using the extended kinetic method. The natural logarithms of the CID product ion ratios, $ln([(BH)^+]/[B_iH^+])$, measured at five collision energies, 1.0, 1.5, 2.0,

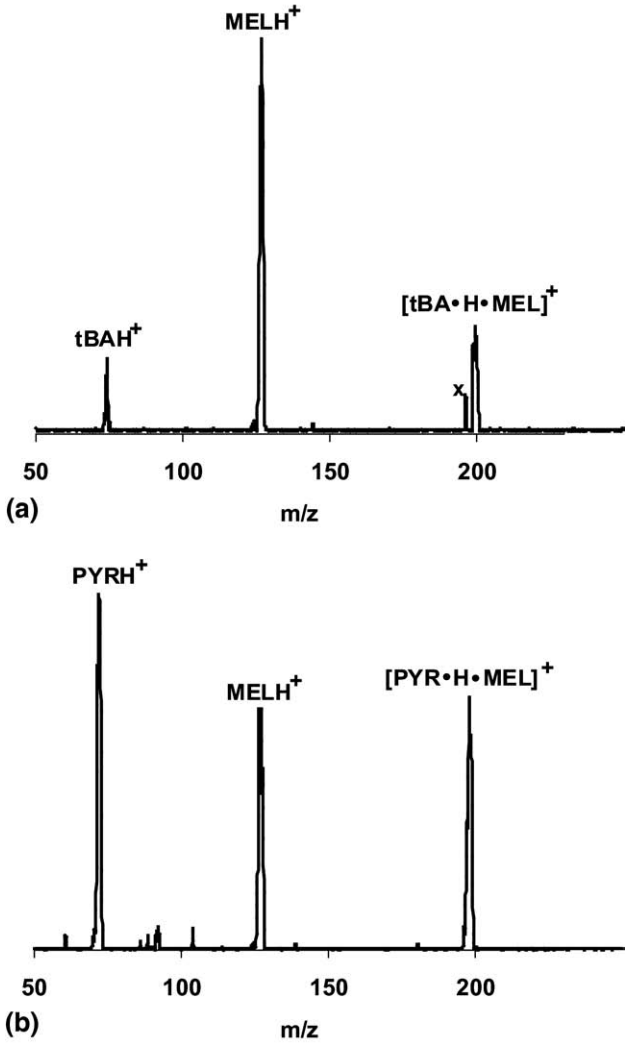

Figure 1. CID spectra obtained at 2.0 eV (E_{cm}) for the proton bound heterodimer anions of (**a**) $[tBA{\cdot}H{\cdot}MEL]^+$ and (**b**) $[PYR{\cdot}H{\cdot}MEL]^+$, where tBA = *t*-butylamine and PYR = pyrrolidine. In (**a**), a noise peak is labeled as x.

Table 2. Values of $ln([BH^+]/[B_iH^+]$[a] measured at five collision energies (E_{cm}) with six references, and the results of linear regression of the first set of the thermo-kinetic plots (eq 2)

B_i	1.0 eV	1.5 eV	2.0 eV	2.5 eV	3.0 eV
Cyclohexylamine	3.17	2.85	2.53	2.34	2.22
t-Butylamine	2.57	2.45	2.30	2.25	2.23
Pyrrolidine	−0.17	−0.08	−0.06	−0.05	−0.08
Diethylamine	−0.98	−0.80	−0.72	−0.69	−0.69
Piperidine	−1.73	−1.50	−1.41	−1.34	−1.34
Dibutylamine	−4.75	−4.26	−3.98	−3.75	−3.46
X	0.93 ± 0.03	0.84 ± 0.03	0.78 ± 0.02	0.74 ± 0.02	0.70 ± 0.02
Y	−0.32 ± 0.10	−0.22 ± 0.08	−0.22 ± 0.07	−0.21 ± 0.05	−0.19 ± 0.06
Z	539 ± 17	597 ± 21	645 ± 17	681 ± 18	719 ± 21

$X = -1/RT_{eff}$.
$Y = [(PA_{MEL} - PA_{avg})/RT_{eff} - \Delta(\Delta S)/R]$.
$Z = T_{eff}$, K.
[a]The data include ±5% of uncertainty.

2.5, and 3.0 eV (E_{cm}), are shown in Table 2, where BH^+ and B_iH^+ represent protonated MEL and reference base, respectively. The secondary fragment ions were insignificant (less than 1%) in this energy range and were not counted in the data analysis. The corresponding thermo-kinetic plots (the first set of the plots) of $ln([BH^+]/[B_iH^+])$ against $(PA_i - PA_{avg})$ are shown in Figure 2a, where PA_{avg} is 226.7 ± 1.6 kcal/mol (Table 1). Linear regression with a least-squares fit of the data points at each collision energy yields a straight line with the slope of $-1/RT_{eff}$ and the y-intercept of $[(PA_{MEL} - PA_{avg})/RT_{eff} - \Delta(\Delta S)/R]$. The slopes and intercepts together with the obtained effective temperatures are summarized in Table 2.

The proton affinity for MEL was derived from the second set of plots. The plot was generated by plotting the values of $y = [(PA_{MEL} - PA_{avg})/RT_{eff} - \Delta(\Delta S)/R]$ obtained from the first set of the plots against the corresponding $1/RT_{eff}$, Figure 2b. Linear regression with a least-squares fit of the data gives a straight line with a slope of −0.49 ± 0.12 kcal/mol $(PA_{MEL} - PA_{avg})$ and an intercept of −0.16 ± 0.10 kcal/mol $(-\Delta(\Delta S)/R)$. Combined with the value of PA_{avg} (226.7 ± 1.6 kcal/mol), the proton affinity of MEL was derived to be 226.2 ± 1.7 kcal/mol. The intercept yields −0.33 ± 0.20 cal/mol K as the value of $\Delta(\Delta S)$. The protonation entropy of MEL (Δ_pS_{MEL}) was calculated using the relationship, $\Delta_pS = \Delta(\Delta S) + \Delta_pS_{avg}$, where Δ_pS_{avg} = 26.9 ± 1.6 cal/mol K (Table 1), and the value of Δ_pS_{MEL} was obtained to be 26.2 ± 1.6 cal/mol K. The uncertainties were calculated by weighted orthogonal distance regression (ODR) using the ODRPACK suite of programs [62]. For example, for each of the plots of $ln([BH^+]/[B_iH^+])$ against $(PA_i - PA_{avg})$, the uncertainty used in all x-axis values is 2.3 kcal/mol, and in all y-axis values it is 0.05. The resulting uncertainties (with 95% confidence) in slope (X) and in intercepts (Y) are shown in Table 2. The corresponding uncertainties were carried into the plot of Y against X. The resulting uncertainty in the slope $(PA_{MEL} - PA_{avg})$ is 0.12 and in the intercept $(\Delta(\Delta S)/R)$ is 0.10. Combined with the 1.6 kcal/mol uncertainty estimated in PA_{avg} (Table 1), the uncertainty in PA_{MEL} would be 1.7 kcal/mol. Considering the uncertainties in the reference bases, we assign ±2.0 kcal/mol for the value of PA_{MEL}, and ±2.0 cal/mol K for the value of Δ_pS_{MEL}. The results are summarized in Table 3. With the proton affinity and the protonation entropy available, we de-

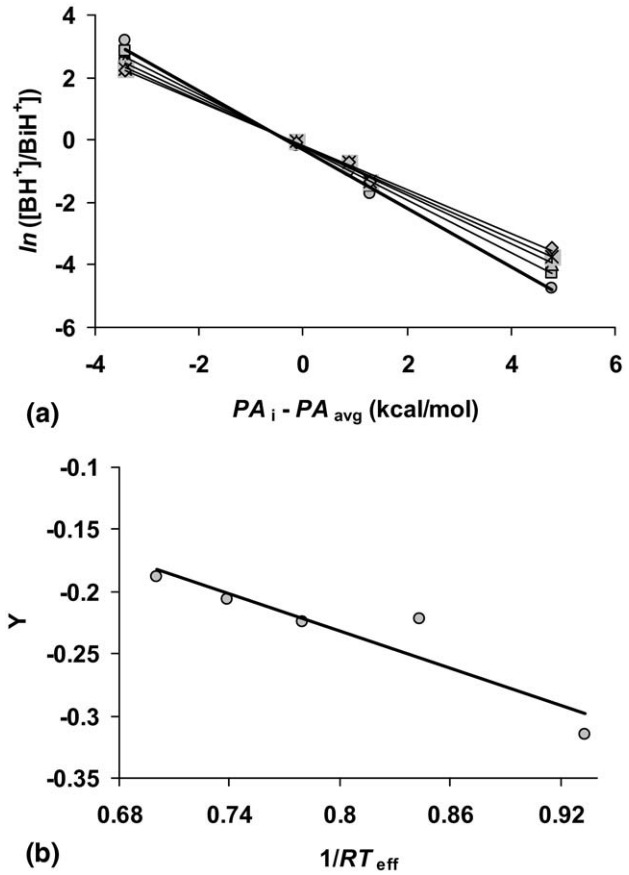

Figure 2. (**a**) Plots of $ln([BH^+]/[B_iH^+]$ against $PA_i - PA_{avg}$ from the dissociation of $[B_i{\cdot}H{\cdot}B]^-$ at five collision energies (E_{cm}), 1.0, 1.5, 2.0, 2.5, and 3.0 eV. The darker line corresponds to the lowest energy data. (**b**) Plots of $Y = [(PA_{MEL} - PA_{avg})/RT_{eff} - \Delta(\Delta S)/R]$ against $1/RT_{eff}$.

Table 3. a) Results of linear regression of the second set of the thermo-kinetic plot (eq 2), and b) the thermochemical quantities of MEL obtained from this work

a)	$PA_{MEL} - PA_{avg}$	$\Delta(\Delta S)/R$	$\Delta(\Delta S)$ (cal/mol K)
	−0.495 ± 0.12	0.165 ± 0.10	−0.33 ± 0.20

b)	PA_{MEL} (kcal/mol)	$\Delta_p S_{MEL}$[a] (cal/mol K)	GB_{MEL}[b] (kcal/mol)
	226.2 ± 2.0 (225.9)[c]	26.2 ± 2.0	218.4 ± 2.0

[a]Estimated using the equation $\Delta_p S = \Delta(\Delta S) + \Delta_p S_{avg}$, where $\Delta_p S_{avg}$ is the average protonation entropy of the reference bases (Table 1).
[b]Derived using eq 3, where T = 298 K.
[c]Calculated using the isodesmic reaction (eq 6) with pyridine as the reference base.

rived the gas-phase basicity of MEL (GB_{MEL}) to be 218.4 ± 2.0 kcal/mol by using eq 3.

Computational Results for Melamine

Two tautomeric forms of melamine were examined. The imide-like triazine-triamine form, **1**, is about 34 kcal/mol more stable than its amide-like tautomer, **2**, at the B3LYP/6-31+G(d) level. Both tautomers have a planar geometry. Protonation at any nitrogen atom does not change the overall geometry. The proton affinity for each type of nitrogen atom in the two tautomeric forms was calculated using the isodesmic proton transfer reaction, eq 6. For tautomer **1**, with using pyridine (PA = 222 kcal/mol) [63] as the reference base, the proton affinity of the triazine nitrogen was calculated to be 225.9 kcal/mol, and with using aniline (PA = 210.9 kcal/mol) [63] as the reference base, the proton affinity of the amino nitrogen was calculated to be 208.5 kcal/mol. The proton affinity of tautomer **2** was calculated using piperidine (PA = 228 kcal/mol) as the reference base. The proton affinities for the nitrogen on the ring and the nitrogen on the side chain are 182.2 kcal/mol and 223.1 kcal/mol, respectively. The stable tautomer of MEL has three NH_2 groups, indicating that MEL also has acidic character, although expected to be weak. The gas-phase deprotonation enthalpy of tautomer 1 (the N-H acidity) was calculated using eq 7 with urea ($\Delta_{acid}H$ = 361.8 ± 2.8 kcal/mol) [63] as the reference acid. The value obtained was 360.5 kcal/mol.

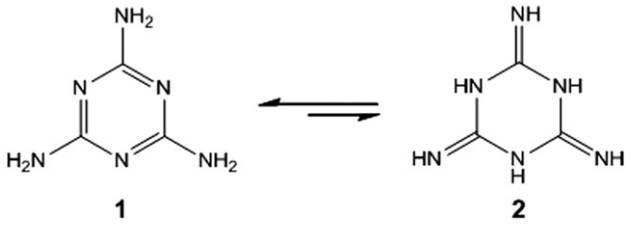

Experimental Results for Cyanuric Acid

Four structurally similar halogenated carboxylic acids (A_iH) were selected as the references: chloroacetic acid ($ClCH_2CO_2H$), bromoacetic acid ($BrCH_2CO_2H$), dibromoacetic acid (Br_2CHCO_2H), and trifluoroacetic acid (F_3CCO_2H), Table 4. The CID bracketing experiments suggest that the acidity of CYA is between those of difluoroacetic acid and dibromoacetic acid. The CID spectra are shown in Figure 3.

The quantitative gas-phase deprotonation enthalpy of CYA ($\Delta_{acid}H_{CYA}$) was measured using the extended kinetic method. For the references containing chlorine and bromine, the proton-bound dimer ions displayed multiple isotope peaks. The most abundant isotope peaks were selected as the precursor ions for the CID experiments. All deprotonated reference acids produced noticeable secondary fragments by losing the CO_2 group at higher collision energies. About 2% of deprotonated CYA also fragmentation further. All secondary fragments were counted in the data analysis. The natural logarithm of ($[A^-]/[A_i^-]$) measured at five collision energies are shown in Table 5, where A^- and A_i^- represent deprotonated CYA and the reference acid, respectively. The corresponding thermo-kinetic plots (the first set of the plots) of $ln([A^-]/[A_i^-])$ against $\Delta_{acid}H_i - \Delta_{acid}H_{avg}$ are shown in Figure 4a, where $\Delta_{acid}H_{avg}$ is 330.9 ± 1.8 kcal/mol (Table 4). Linear regression with a least-squares fit of the data points at each collision energy yielded a straight line with the slope of $1/RT_{eff}$ and the y-intercept of $-[(\Delta_{acid}H_{CYA} - \Delta_{acid}H_{avg})/RT_{eff} - \Delta(\Delta S)/R]$. The slopes and intercepts together with the effective temperatures derived from the linear regression are summarized in Table 5.

The value of $\Delta_{acid}H_{CYA}$ was derived from the second set of the plot. The plot was generated by plotting the

Table 4. Thermochemical quantities of the reference acids used for the cyanuric system

Reference base	$\Delta_{acid}H$[a]	$\Delta_{acid}G$[a]	$\Delta_{acid}S$[b]
	(kcal/mol)	(kcal/mol)	(cal/mol K)
Bromoacetic acid	334.8 ± 2.3	328.2 ± 2.0	22.1
Difluoroacetic acid	331 ± 2.2	323.8 ± 2.0	24.2
Dibromoacetic acid	328.3 ± 2.2	321.3 ± 2.0	23.5
Trifluoroacetic acid	323.8 ± 2.9	317.4 ± 2.0	21.5
	$\Delta_{acid}H_{avg}$ = 330.9 ± 1.8[c]		$\Delta_{acid}S_{avg}$ = 22.8 ± 1.8[d]

[a]Obtained from the NIST Chemistry Webbook [63].
[b]Derived from $\Delta_{acid}H$ and $\Delta_{acid}G$: $\Delta_{acid}G = \Delta_{acid}H - T(\Delta_{acid}S)$, where T = 298 K and $\Delta_{acid}S$ is assumed to have 2.0 cal/mol K uncertainty.
[c]Average deprotonation enthalpy of the set of reference acids.
[d]Average deprotonation entropy of the set of reference acids.

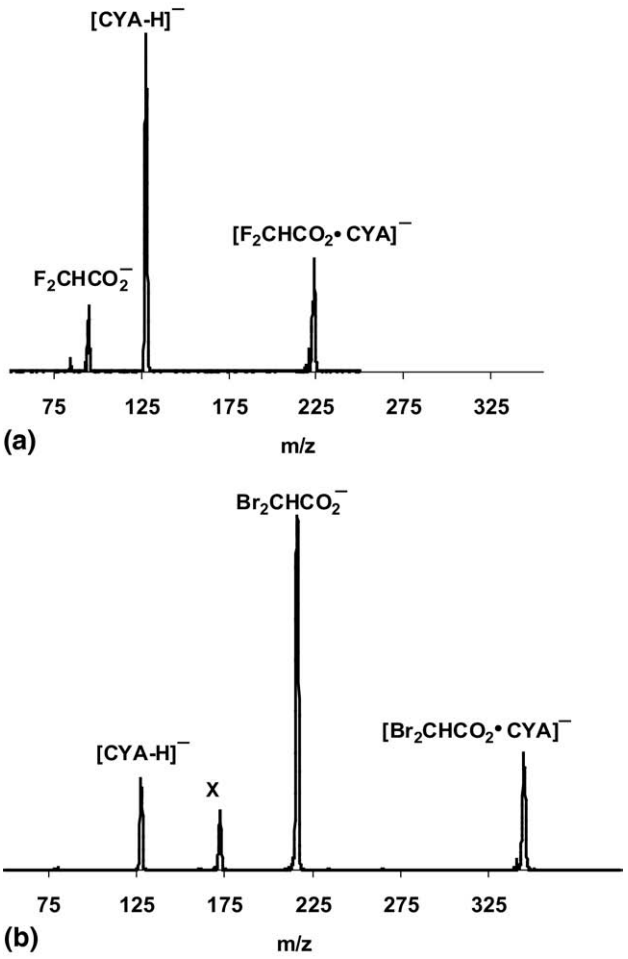

Figure 3. CID spectra obtained at 2.0 eV (E_{cm}) for the proton bound heterodimer anions of (**a**) $[F_2CHCO_2{\cdot}CYA]^-$ and b) $[Br_2CHCO_2{\cdot}CYA]^-$. In (**b**) the peak at X corresponds to the secondary fragment from the ion of $Br_2CHCO_2^-$.

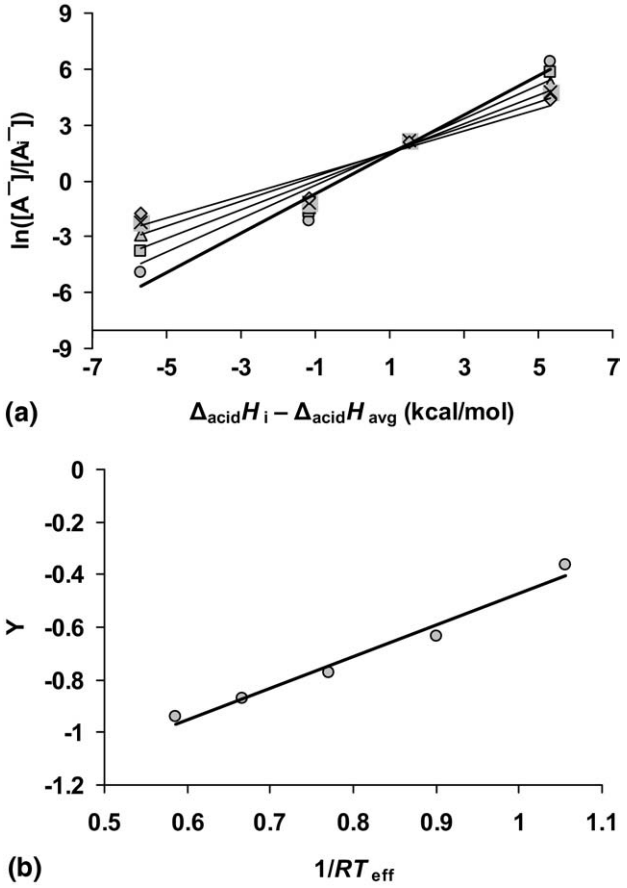

Figure 4. (**a**) Plots of $\ln([A^-]/[A_i^-])$ against $\Delta_{acid}H_i - \Delta_{acid}H_{avg}$ from the dissociation of $[A_i{\cdot}H{\cdot}A]^-$ at five collision energies (E_{cm}), 1.0, 1.5, 2.0, 2.5, and 3.0 eV. The darker line corresponds to the lowest energy data. (**b**) Plots of $Y = (\Delta_{acid}H - \Delta_{acid}H_{avg})/RT_{eff} - \Delta(\Delta S)/R$ against $1/RT_{eff}$.

values of $y = [(\Delta_{acid}H_{CYA} - \Delta_{acid}H_{avg})/RT_{eff} - \Delta(\Delta S)/R]$ obtained from the first set of the plots against the corresponding $1/RT_{eff}$, Figure 4b. Linear regression with a least-squares fit gave a straight line with a slope of 1.23 ± 0.11 ($\Delta_{acid}H_{CYA} - \Delta_{acid}H_{avg}$) and an intercept of −1.70 ± 0.09 ($-\Delta(\Delta S)/R$). Combined with $\Delta_{acid}H_{avg}$, the value of $\Delta_{acid}H_{CYA}$ was derived to be 330.7 ± 1.8 kcal/mol. The intercept gave the value of $\Delta(\Delta S)$ to be 3.33 ± 0.18 cal/mol K. The deprotonation entropy of CYA ($\Delta_{acid}S_{CYA}$) was calculated to be 26.1 ± 1.8 cal/mol K by using the relationship $\Delta_{acid}S = \Delta(\Delta S) + \Delta_{acid}S_{avg}$, where $\Delta_{acid}S_{avg}$ = 22.8 ± 1.8 cal/mol K (Table 4). Considering the uncertainties in the reference acids, we assign ±2.0 kcal/mol for $\Delta_{acid}H_{CYA}$, and ±2.0 cal/mol

Table 5. Values of $\ln([\bar{A}]/[A_i^-])$[a] measured at five collision energies (E_{cm}) with four reference acids, and the results of linear regression of the first set of the thermo-kinetic plots (eq 4)

A_iH	1.0 eV	1.5 eV	2.0 eV	2.5 eV	3.0 eV
Bromoacetic acid	6.39	5.83	5.24	4.75	4.36
Difluoroacetic acid	2.14	2.18	2.17	2.16	2.10
Dibromoacetic acid	−2.14	−1.69	−1.39	−1.15	−0.91
Trifluoroacetic acid	−4.95	−3.78	−2.92	−2.28	−1.79
X′	1.05 ± 0.13	0.90 ± 0.13	0.77 ± 0.13	0.67 ± 0.13	0.59 ± 0.12
Y′	−0.36 ± 0.53	−0.63 ± 0.53	−0.77 ± 0.53	−0.87 ± 0.51	−0.94 ± 0.48
Z′	476 ± 59	558 ± 81	653 ± 110	754 ± 146	858 ± 175

X′ = $1/RT_{eff}$.
Y′ = $[(\Delta_{acid}H - \Delta_{acid}H_{avg})/RT_{eff} - \Delta(\Delta S)/R]$.
Z′ = T_{eff}, K.
[a]The data include ±5% of uncertainty.

Table 6. a) Results of linear regression of the second set of the thermo-kinetic plot (eq 4), and b) the thermochemical quantities of CYA obtained from this work

a)	$\Delta_{acid}H_{CYA}$-$\Delta_{acid}H_{avg}$ (kcal/mol)	$\Delta(\Delta S)/R$	$\Delta(\Delta S)$ (cal/mol K)
	1.23 ± 0.11	−1.70 ± 0.09	3.33 ± 0.18
b)	$\Delta_{acid}H_{CYA}$ (kcal/mol)	ΔS_{CYA}[a] (cal/mol K)	$\Delta_{acid}G_{CYA}$[b] (kcal/mol)
	330.7 ± 2.0 (328.4)[c]	26.1 ± 2.0	322.9 ± 2.0

[a]Estimated using the equation $\Delta_{acid}S = \Delta(\Delta S) + \Delta_{acid}S_{avg}$, where $\Delta_{acid}S_{avg}$ is the average deprotonation entropy of the reference acids (Table 1).
[b]Derived using eq 5, where T = 298 K.
[c]Calculated using the isodesmic reaction (eq 7) with urea as the reference.

K for $\Delta_{acid}S_{CYA}$. Finally, the gas-phase acidity of CYA ($\Delta_{acid}G_{CYA}$) was derived to be 322.9 ± 2.0 kcal/mol by using eq 5. The results are summarized in Table 6.

Computational Results for Cyanuric Acid

The structures and energies of the two tautomers of CYA were calculated at the B3LYP/6-31+G(d) level. The keto-like tautomer, **4**, is more stable than the enol-like triazine-triol form, **3**, by 33 kcal/mol. Both forms have a planar geometry. Abstraction of any proton does not change the overall planar geometry. The gas-phase deprotonation enthalpy of tautomer **4** (the N–H bond acidity) was calculated to be 328.4 kcal/mol by using the eq 7 with urea ($\Delta_{acid}H$ = 361.8 ± 2.8 kcal/mol) [63] as the reference. The deprotonation enthalpy of tautomer **3** (the O-H bond acidity) was calculated to be 329.2 kcal/mol with phenol ($\Delta_{acid}H$ = 350 ± 2 kcal/mol) [63] as the reference acid. CYA may also function as a base. The proton affinity of tautomer **4** was calculated using eq 6. The proton affinity at the oxygen was given to be 163.2 kcal/mol with cyclohexanone (PA = 210. kcal/mol) [63] as the reference base. With piperidine as the reference, the proton affinity at the nitrogen was given to be 181.5 kcal/mol.

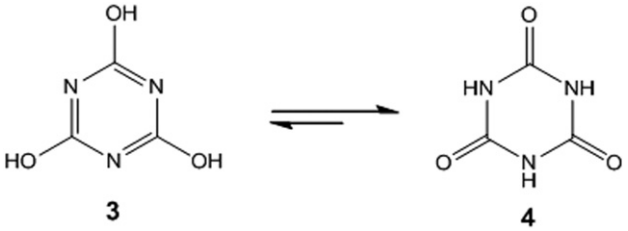

3 **4**

Discussion

Computational studies clearly show that in the gas-phase the imide-like triazine-triamine tautomer (**1**) is energetically more favored for MEL, while the keto-like tautomer (**4**) is energetically more favored for CYA. Early studies by X-ray crystallography and ultraviolet absorption experiments also suggested that MEL and CYA could be represented best by the imide-like and keto-like tautomers, respectively, in both the solid state and in solution [64]. The differences in the preference for the tautomeric forms can be understood by considering the energies involved in the tautomerization. The conversion from the imide-like form to the amide-like form in MEL merely trades one C=N for another, and the tautomerization is about thermal neutral. The resonance energy gained in the imide-like form makes this tautomer more favored than the amide-like form. While in the tautomerization of CYA from the enol-like form (**3**) to the keto-like one (**4**), the three *N*=C-OH connections are converted to three HN-C=O connections. It has been estimated that the tautomerization form *N*=C-OH to HN-C=O is exothermic by about 10 kcal/mol. The conversion from tautomer **3** to tautomer **4** is accompanied by a stabilization energy of about 30 kcal/mol. This energy is sufficient to overcome the resonance energy in the triazine ring [64, 65].

The proton affinity and the gas-phase basicity of MEL were determined to be 226.2 ± 2.0 kcal/mol and 218.4 ± 2.0 kcal/mol, respectively. In either of the two tautomers, there are two possible protonation sites, the nitrogen on the ring and the nitrogen on the outside of the ring. Theoretically predicted proton affinities are quite different for these nitrogen atoms. In the more stable tautomer, **1**, the calculated proton affinity for the triazine nitrogen is 225.9 kcal/mol and for the amino group nitrogen is 208.5 kcal/mol. The former value is in good agreement with the experimental result. Apparently the triazine nitrogen is more basic than the primary amino group nitrogen. This is reasonable based on the general understanding of the heterocyclic aromatic systems. The lone pair of electrons on the amino nitrogen is largely delocalized into the aromatic ring system, while the lone pair on the triazine nitrogen is largely localized on the nitrogen atom. The electron delocalization effect on the proton affinity is clearly seen in the case of aniline versus pyridine. The proton affinity of pyridine (222 kcal/mol) is about 10 kcal/mol stronger than that of aniline (210.9 kcal/mol). The proton affinity of MEL is also higher than that of pyridine. This can be explained by electron donating effect from the three amino groups in MEL, which would increase the electron density on the triazine nitrogen.

The kinetic method yielded the protonation enthalpy and the gas-phase acidity of CYA to be 330.7 ± 2.0 kcal/mol and 322.9 ± 2.0 kcal/mol, respectively. CYA is a slightly stronger acid than difluoroacetic acid. Theoretically the N–H bond in the keto-like tautomer **4** (329.2 kcal/mol) has a comparable deprotonation enthalpy to the O–H bond in the enol-like tautomer **3** (328.4 kcal/mol). Both values agree well with the experimental value. Since tautomer **4** is energetically more favored and is likely the only form in the gas phase, the measured deprotonation enthalpy reflects that for the N–H bond in tautomer **4**.

Can MEL be used as an acid and CYA be used as a base? The three NH_2 groups in **1** indicate that MEL has acidic character. Computational studies suggest that MEL is a weak acid and has the acidity comparable to that of urea in the gas-phase. CYA has two basic sites, the oxygen and the nitrogen. In tautomer **4**, the nitrogen is about 20 kcal/mol more basic than the oxygen. Computational studies suggest that CYA is a weak base with the basicity comparable to that of pentafluoropyridine (PA = 182.8 kcal/mol) [63].

The derived protonation entropy for MEL, 26.2 cal/mol K, is about the same as those of the reference bases (Table 1). The obtained deprotonation entropy for CYA, 26.1 cal/mol K, is about 3 cal/mol K higher than those of the reference acids (Table 4). MEL and CYA have a similar geometry. Addition or abstraction of a proton does not change the rigid planar geometry. Therefore, it is expected that the protonation entropy for MEL and the deprotonation entropy for CYA should be about the same. The set of reference bases used in the MEL system are primary and secondary amines, and they all have relatively rigid structures. It is not surprising that the protonation entropy for MEL is comparable to those of these amines. The structures of the group of reference acids used in the CYA system are relatively flexible. Upon deprotonation, small geometry changes are expected, and these changes would result in a slightly more compacted geometry and, hence, a reduced entropy. It is reasonable that the deprotonation entropies of the references are slightly lower than that of CYA.

Conclusions

We have determined the gas-phase thermochemical quantities of melamine and cyanuric acid using the extended kinetic method along with computational studies. MEL is a stronger base than pyridine. The proton affinity, gas-phase basicity, and protonation entropy for MEL were determined to be $PA = 226.2 \pm 2.0$ kcal/mol, $GB = 218.4 \pm 2.0$ kcal/mol, and $\Delta_pS = 26.2 \pm 2.0$ cal/mol K, respectively. CYA is a slightly stronger acid than difluoroacetic acid. The deprotonation enthalpy, gas-phase acidity, and deprotonation entropy for CYA were determined to be $\Delta_{acid}H = 330.7 \pm 2.0$ kcal/mol, $\Delta_{acid}G = 322.9 \pm 2.0$ kcal/mol, and $\Delta_{acid}S = 26.1 \pm 2.0$ cal/mol K, respectively. The computationally predicted proton affinity of MEL (225.9 kcal/mol) and gas-phase deprotonation enthalpy of CYA (328.4 kcal/mol) agree well with the experimental results. In addition, MEL also has an acidic character and CYA has a basic character. MEL is a weak acid comparable to urea, and CYA is a weak base comparable to pentafluoropyridine. MEL is best represented as the imide-like triazine-triamine form, and the triazine nitrogen is more basic than the amino group nitrogen. CYA is best represented as the keto-like tautomer and the N-H group is the most possible proton donor.

Acknowledgments

The authors acknowledge partial support of this research by the National Science Foundation (CHE-0749737). The instrument usage was provided by the Mass Spectrometry Facility at the University of the Pacific.

References

1. Palanikkumaran, M.; Gupta, K. K.; Agrawal, A. K.; Jassal, M. Highly Stable Hexamethylolmelamine Microcapsules Containing N-Octadecane Prepared by In Situ Encapsulation. *J. Appl. Polym. Sci.* **2009,** *114,* 2997–3002.
2. Pavlyuchenko, V. N.; Ivanchev, S. S.; Ratzsch, M.; Bucka, H.; Primachenko, O. N.; Leitner, P.; Khaikin, S. Y. Transetherification of Melamine-Formaldehyde Resin Methyl Ethers and Competing Reaction of Self-Condensation. *J. Appl. Polym. Sci.* **2006,** *101,* 2977–2985.
3. Lefebvre, J.; Le Bras, M.; Bastin, B.; Paleja, R.; Delobel, R. Flexible Polyurethane Foams: Flammability. *J. Fire Sci.* **2003,** *21,* 343–367.
4. Hainz, R.; Allaz, J.; Schroeder, D. Isometric Isoindoline Yellow Pigments Used in Paints; (Ciba Holding Inc., Switz.; BASF SE). In *PCT Int. Appl.;* Application: WO 2009074533, 2009, p. 36.
5. Scarpato, M. Substrate Having a Surface Printed by Digital Printing, and Digital Printing Method; (Microtek S.r.l., Italy). In *PCT Int. Appl.;* Application: WO 2007096912, 2007, p. 27.
6. Lim, L. O.; Scherer, S. J.; Shuler, K. D.; Toth, J. P. Disposition of Cyromazine in Plants Under Environmental Conditions. *J. Agric. Food Chem.* **1990,** *38,* 860–864.
7. Sancho, J. V.; Ibanez, M.; Grimalt, S.; Pozo, O. J.; Hernandez, F. Residue Determination of Cyromazine and Its Metabolite Melamine in Chard Samples by Ion-Pair Liquid Chromatography Coupled to Electrospray Tandem Mass Spectrometry. *Anal. Chim. Acta* **2005,** *530,* 237–243.
8. Hauck, R. D.; Stephenson, H. F. Nitrification of Triazine Nitrogen. *J. Agric. Food Chem.* **1964,** *12,* 147–151.
9. Zaknich, A. Swimming Pool and Spa Water Testing Process; Granted Innovation Pat. (Australia). Application: AU 2009100474, 2009, p. 8.
10. Teichberg, V. I. Methods and Compositions and Devices for Maintaining Chemical Balance of Chlorinated Water; (Yeda Research and Development Co. Ltd., Israel). In *PCT Int. Appl.;* Application: WO 2007107981, 2007, p. 58.
11. Whitesides, G. M.; Mathias, J. P.; Seto, C. T. Molecular Self-Assembly and Nanochemistry: A Chemical Strategy for the Synthesis of Nanostructures. *Science* **1991,** *254,* 1312–1319.
12. Arduini, M.; Crego-Calama, M.; Timmerman, P.; Reinhoudt, D. N. A Novel Type of Hydrogen-Bonded Assemblies Based on the Melamine-Cyanuric Acid Motif. *J. Org. Chem.* **2003,** *68,* 1097–1106.
13. Perdigao, L. M. A.; Champness, N. R.; Beton, P. H. Surface Self-Assembly of the Cyanuric Acid-Melamine Hydrogen Bonded Network. *Chem. Commun.* (Cambridge, UK) **2006,** 538–540.
14. Ranganathan, A.; Pedireddi, V. R.; Rao, C. N. R. Hydrothermal Synthesis of Organic Channel Structures: 1:1 Hydrogen-Bonded Adducts of Melamine with Cyanuric and Trithiocyanuric Acids. *J. Am. Chem. Soc.* **1999,** *121,* 1752–1753.
15. Damodaran, K.; Sanjayan, G. J.; Rajamohanan, P. R.; Ganapathy, S.; Ganesh, K. N. Solid State NMR of a Molecular Self-Assembly: Multinuclear Approach to the Cyanuric Acid-Melamine System. *Org. Lett.* **2001,** *3,* 1921–1924.
16. Lam, C. W.; Lan, L.; Che, X.; Tam, S.; Wong, S. S. Y.; Chen, Y.; Jin, J.; Tao, S. H.; Tang, X. M.; Yuen, K. Y.; Tam, P. K.-H. Diagnosis and Spectrum of Melamine-Related Renal Disease: Plausible Mechanism of Stone Formation in Humans. *Clin. Chim. Acta* **2009,** *402,* 150–155.
17. Dobson, R. L. M.; Motlagh, S.; Quijano, M.; Cambron, R. T.; Baker, T. R.; Pullen, A. M.; Regg, B. T.; Bigalow-Kern, A. S.; Vennard, T.; Fix, A.; Reimschuessel, R.; Overmann, G.; Shan, Y.; Daston, G. P. Identification and Characterization of Toxicity of Contaminants in Pet Food Leading to an Outbreak of Renal Toxicity in Cats and Dogs. *Toxicol. Sci.* **2008,** *106,* 251–262.
18. Puschner, B.; Poppenga Robert, H.; Lowenstine Linda, J.; Filigenzi Michael, S.; Pesavento Patricia, A. Assessment of Melamine and Cyanuric Acid Toxicity in Cats. *J. Vet. Diagn. Invest.* **2007,** *19,* 616–624.
19. Tang, H. W.; Ng, K. M.; Chui, S. S. Y.; Che, C. M.; Lam, C. W.; Yuen, K. Y.; Siu, T. S.; Lan, L. C. L.; Che, X. Analysis of Melamine Cyanurate in Urine Using Matrix-Assisted Laser Desorption/Ionization Mass Spectrometry. *Anal. Chem.* (Washington, DC) **2009,** *81,* 3676–3682.
20. Zhu, L.; Gamez, G.; Chen, H.; Chingin, K.; Zenobi, R. Rapid Detection of Melamine in Untreated Milk and Wheat Gluten by Ultrasound-Assisted Extractive Electrospray Ionization Mass Spectrometry (EESI-MS) *Chem. Commun.* (Cambridge, UK) **2009,** 559–561.
21. Huang, G.; Ouyang, Z.; Cooks, R. G. High-Throughput Trace Melamine Analysis in Complex Mixtures. *Chem. Commun.* (Cambridge, UK) **2009,** 556–558.
22. Andersen, W. C.; Turnipseed, S. B.; Karbiwnyk, C. M.; Clark, S. B.; Madson, M. R.; Gieseker, C. M.; Miller, R. A.; Rummel, N. G.; Reimschuessel, R. Determination and Confirmation of Melamine Residues in Catfish, Trout, Tilapia, Salmon, and. Shrimp by Liquid Chromatography with Tandem Mass Spectrometry. *J. Agric. Food Chem.* **2008,** *56,* 4340–4347.

23. Vail, T. M.; Jones, P. R.; Sparkman, O. D. Rapid and Unambiguous Identification of Melamine in Contaminated Pet Food Based on Mass Spectrometry with Four Degrees of Confirmation. *J. Anal. Toxicol.* **2007,** *31,* 304–312.
24. Heller, D. N.; Nochetto, C. B. Simultaneous Determination and Confirmation of Melamine and Cyanuric Acid in Animal Feed by Zwitterionic Hydrophilic Interaction Chromatography and Tandem Mass Spectrometry. *Rapid Commun. Mass Spectrom.* **2008,** *22,* 3624–3632.
25. Lin, M.; He, L.; Awika, J.; Yang, L.; Ledoux, D. R.; Li, H.; Mustapha, A. Detection of Melamine in Gluten, Chicken Feed, and Processed Foods Using Surface Enhanced Raman Spectroscopy and HPLC. *J. Food Sci.* **2008,** *73,* T129–134.
26. Ai, K.; Liu, Y.; Lu, L. Hydrogen-Bonding Recognition-Induced Color Change of Gold Nanoparticles for Visual Detection of Melamine in Raw Milk and Infant Formula. *J. Am. Chem. Soc.* **2009,** *131,* 9496–9497.
27. Rapid detection of melamine in dry milk using AccuTOF-DART; Application Note: MS-0810, JEOL, 2008.
28. "A Rapid and Sensitive Method for the Simultaneous Determination of Melamine and Cyanuric Acid in Infant Formulas, Adult Nutritional products, and Protein Powers; Application Note: 720002889en, Waters, 2009.
29. Taylor, A.; Sakuma, T.; Schreiber, A. A New, Fast, and Sensitive LC/MS/MS Method for the Accurate Quantitation and Confirmation of Melamine and Cyanuric Acid in Pet Food Samples; Application Note: Melamine and Cyanuric Acid, 114AP62-02, Applied Biosystemes/MDS SCIEX, 2008.
30. Fremlin, L. J.; Pelzing, M. Melamine and Cyanuric Acid Detection in 5 Minutes Using LCMS; Application Note: LCMS-49, Bruker Daltonics, 2008.
31. Varelis, P.; Beck, J.; Wang, K.; Ghosh, D. Analysis of Melamine and Cyanuric Acid in Food Matrices by LC-MS-MS; Application Note: 424, Thermo Fisher Scientific, 2008.
32. Liu, P.; Xiong, W.; Hu, S. Z.; Li, X.; Tan, Z. -C. Enthalpy of Formation, Heat Capacity, and Entropy of Melamine. *Wuli Huaxue Xuebao* **2009,** *25,* 2417–2421.
33. He, Y.; Liu, X.; Lin, M. C.; Melius, C. F. Thermal Reaction of Isocyanic acid with Nitrogen Dioxide at Moderate Temperatures. *Int. J. Chem. Kinet.* **1993,** *25,* 845–863.
34. De Wit, H. G. M.; De Kruif, C. G.; Van Miltenburg, J. C. Thermodynamic Properties of Molecular Organic Crystals Containing Nitrogen, Oxygen, and Sulfur. II. Molar Heat Capacities of Eight Compounds by Adiabatic Calorimetry. *J. Chem. Thermodyn.* **1983,** *15,* 891–902.
35. Vollhardt, D.; Fainerman, V. B.; Liu, F. Thermodynamic and Structural Characterization of Amphiphilic Melamine-Type Monolayers. *J. Phys. Chem. B* **2005,** *109,* 11706–11711.
36. Cooks, R. G.; Patrick, J. S.; Kotiaho, T.; McLuckey, S. A. Thermochemical Determinations by the Kinetic Method. *Mass Spectrom. Rev.* **1994,** *13,* 287–339.
37. Cooks, R. G.; Wong, P. S. H. Kinetic Method of Making Thermochemical Determinations: Advances and Applications. *Acc. Chem. Res.* **1998,** *31,* 379–386.
38. Cooks, R. G.; Koskinen, J. T.; Thomas, P. D. The Kinetic Method of Making Thermochemical Determinations. *J. Mass Spectrom.* **1999,** *34,* 85–92.
39. Cheng, X.; Wu, Z.; Fenselau, C. Collision Energy Dependence of Proton-Bound Dimer Dissociation: Entropy Effects, Proton Affinities, and Intramolecular Hydrogen-Bonding in Protonated Peptides. *J. Am. Chem. Soc.* **1993,** *115,* 4844–4848.
40. Cerda, B. A.; Wesdemiotis, C. Li+, Na+, and K+ Binding to the DNA and RNA Nucleobases, Bond Energies and Attachment Sites from the Dissociation of Metal Ion-Bound Heterodimers. *J. Am. Chem. Soc.* **1996,** *118,* 11884–11892.
41. Bouchoux, G.; Sablier, M.; Berruyer-Penaud, F. Obtaining Thermochemical Data by the Extended Kinetic Method. *J. Mass Spectrom.* **2004,** *39,* 986–997.
42. Bouchoux, G.; Desaphy, S.; Bourcier, S.; Malosse, C.; Bimbong, R. N. B. Gas-Phase Protonation Thermochemistry of Arginine. *J. Phys. Chem. B* **2008,** *112,* 3410–3419.
43. Bouchoux, G.; Bimbong, R. N. B.; Nacer, F. Gas-Phase Protonation Thermochemistry of Glutamic. *Acid J. Phys. Chem. A* **2009,** *113,* 6666–6676.
44. Zheng, X.; Cooks, R. G. Thermochemical Determinations by the Kinetic Method with Direct Entropy Correction. *J. Phys. Chem. A* **2002,** *106,* 9939–9946.
45. Schroeder, O. E.; Andriole, E. J.; Carver, K. L.; Colyer, K. E.; Poutsma, J. C. Proton Affinity of Lysine Homologues from the Extended Kinetic Method. *J. Phys. Chem. A* **2004,** *108,* 326–332.
46. Harrison, A. G. The Gas-Phase Basicities and Proton Affinities of Amino Acids and Peptides. *Mass Spectrom. Rev.* **1997,** *16,* 201–217.
47. Kaltashov, I. A.; Fabris, D.; Fenselau, C. C. Assessment of Gas Phase Basicities of Protonated Peptides by the Kinetic Method. *J. Phys. Chem.* **1995,** *99,* 10046–10051.
48. Jones, C. M.; Bernier, M.; Carson, E.; Colyer, K. E.; Metz, R.; Pawlow, A.; Wischow, E. D.; Webb, I.; Andriole, E. J.; Poutsma, J. C. Gas-Phase Acidities of the 20 Protein Amino Acids. *Int. J. Mass Spectrom.* **2007,** *267,* 54–62.
49. Fournier, F.; Afonso, C.; Fagin, A. E.; Gronert, S.; Tabet, J.-C. Can Cluster Structure Affect Kinetic Method Measurements? The Curious Case of Glutamic Acid's Gas-Phase Acidity. *J. Am. Soc. Mass Spectrom.* **2008,** *19,* 1887–1896.
50. Ren, J.; Tan, J. P.; Harper, R. T. Gas-Phase Acidities of Cysteine-Polyalanine peptides I: A3,4CSH and HSCA3,4. *J. Phys. Chem. A* **2009**, *113,* 13903–10912.
51. Drahos, L.; Peltz, C.; Vekey, K. Accuracy of Enthalpy and Entropy Determination Using the Kinetic Method: Are We Approaching a Consensus? *J. Mass Spectrom.* **2004,** *39,* 1016–1024.
52. Laskin, J.; Futrell, J. H. The Theoretical Basis of the Kinetic Method from the Point of View of Finite Heat Bath Theory. *J. Phys. Chem. A* **2000,** *104,* 8829–8837.
53. Ervin, K. M. Microcanonical Analysis of the Kinetic Method. The Meaning of the "Apparent Entropy." *J. Am. Soc. Mass Spectrom.* **2002,** *13,* 435–452.
54. Meot-Ner, M.; Somogyi, A. A Thermal Extrapolation Method for the Effective Temperatures and Internal Energies of Activated Ions. *Int. J. Mass Spectrom.* **2007,** *267,* 346–356.
55. Armentrout, P. B. Entropy Measurements and the Kinetic Method: a Statistically Meaningful Approach. *J. Am. Soc. Mass Spectrom.* **2000,** *11,* 371–379.
56. Ervin, K. M.; Armentrout, P. B. Systematic and Random Errors in Ion Affinities and Activation Entropies from the Extended Kinetic Method. *J. Mass Spectrom.* **2004,** *39,* 1004–1015.
57. Frisch, M. J.; Trucks, G. W.; Schlegel, H. B.; Scuseria, G. E.; Robb, M. A.; Cheeseman, J. R.; Montgomery, J. A. Jr.; Vreven, T.; Kudin, K. N.; Burant, J. C.; Millam, J. M.; Iyengar, S. S.; Tomasi, J.; Barone, V.; Mennucci, B.; Cossi, M.; Scalmani, G.; Rega, N.; Petersson, G. A.; Nakatsuji, G.; Hada, M.; Ehara, M.; Toyota, K.; Fukuda, R.; Hasegawa, J.; Ishida, M.; Nakajima, T.; Honda, Y.; Kitao, O.; Nakai, H.; Klene, M.; Li, X.; Knox, J. E.; Hratchian, H. P.; Cross, J. B.; Adamo, C.; Jaramillo, J.; Gomperts, R.; Stratmann, R. E.; Yazyev, O.; Austin, A. J.; Cammi, R.; Adamo, C.; Jaramillo, J.; Gomperts, R.; Stratmann, R. E.; Yazyev, O.; Austin, A. J.; Cammi, R.; Pomelli, C.; Ochterski, J. W.; Ayala, P. Y.; Morokuma, K.; Voth, G. A.; Salvador, P.; Dannenberg, J. J.; Zakrzewski, V. G.; Dapprich, S.; Daniels, A. D.; Strain, M. C.; Farkas, O.; Malick, D. K.; Rabuck, A. D.; Raghavachari, K.; Foresman, J. B.; Ortiz, J. V.; Cui, Q.; Baboul, A. G.; Clifford, S.; Cioslowski, J.; Stefanov, B. B.; Liu, G.; Liashenko, A.; Piskorz, P.; Komaromi, I.; Martin, R. L.; Fox, D. J.; Keith, T.; Al-Laham, M. A.; Peng, C. Y.; Nanayakkara, A.; Challacombe, M.; Gill, P. M. W.; Johnson, B.; Chen, W.; Wong, M. W.; Gonzalez, C.; Pople, J. A. *Gaussian 03, Revision A 1*; Gaussian, Inc.: Pittsburgh PA, 2003.
58. Parr, R. G.; Yang, W. *Density-Functional Theory of Atoms and Molecules*; Clarendon Press: New York, 1989; p. 333.
59. Becke, A. D. Density-Functional Exchange-Energy Approximation with Correct Asymptotic Behavior. *Phys. Rev. A* **1988,** *38,* 3098–3100.
60. Becke, A. D. Density-Functional Thermochemistry. III. The Role of Exact Exchange *J. Chem. Phys.* **1993,** *98,* 5648–5652.
61. Lee, C.; Yang, W.; Parr, R. G. Development of the Colle-Salvetti Correlation-Energy Formula into a Functional of the Electron Density. *Phys. Rev. B* **1988,** *37,* 785–789.
62. Boggs, P. T.; Byrd, R. H.; Rogers, J. E.; Schnabel, R. B. ODRPACK Version 2.01 Software for Weighted Orthogonal Distance Regression Report NISTIR 92-4834. National Institute of Standards and Technology: Gaithersburg, MD, 1992.
63. *NIST Chemistry WebBook, NIST Standard Reference Database Number* 69; Linstrom, P. J.; Mallard, W. G., Eds.; National Institute of Standards and Technology: Gaithersburg MD; http://webbook.nist.gov.
64. Klotz, I. M.; Askounis, T. Absorption Spectra and Tautomerism of Cyanuric Acid, Melamine, and Some Related Compounds. *J. Am. Chem. Soc.* **1947,** *69,* 801–803.
65. Liang, X.; Pu, X.; Zhou, H.; Wong, N. B.; Tian, A. Keto-Enol Tautomerization of Cyanuric Acid in the Gas Phase and in Water and Methanol. *THEOCHEM* **2007,** *816,* 125–136.